

Templated Cross-linked Nanoporous Starch

Somayeh Oftadehgan^a, Ahmad Poursattar Marjani^{a,*} and Asghar Zamani^{b,*}

^aDepartment of Organic Chemistry, Faculty of Chemistry, Urmia University, Urmia, Iran.

^bDepartment of Nanotechnology, Faculty of Science, Urmia University, Urmia, Iran.

Received 8 May 2020, revised 12 July 2020, accepted 21 July 2020.

ABSTRACT

Nanoporous starch materials were successfully prepared by a sustainable synthetic process. In this method, some available economic cationic, anionic and nonionic templates like CTAB, SDS and Tween 80 in the presence of borax, as a green and low-cost cross-linker, were used to synthesize the desired cross-linked nanoporous starch in the aqueous phase at relatively low temperature. The obtained materials were characterized by SEM, FT-IR, TGA, DSC and N₂ adsorption/desorption methods. While SEM analysis confirmed the porous nature of the materials, BET measurement showed that the materials can have a specific surface area of 65 m² g⁻¹. Cross-linked nanoporous starch was found to be an efficient, inexpensive, easy to prepare, green adsorbent in the removal of methylene blue and methyl orange from wastewater. The synthesized material was found to be highly efficient in controlled adsorption and desorption of ciprofloxacin, which can be applied in drug delivery.

KEYWORDS

Starch, surface area, cross-linker, nanoporous materials, drug delivery, dye removal.

1. Introduction

Over the past few years, investigation of bio-based plastics has been done because of their potential biocompatibility for eco-friendly protection and also a decrease in the production and use of non-degradable plastic.¹ The substitution and removal of petro-based polymers have directed the interest of many researchers toward the application of starch-derived plastic.²

Starch is a vital component of human nutrition.³ Usually, it is extracted from cassava, tapioca, potatoes, corn, wheat and rice. Starch is generally used in the native form but due to its inadequate stability, it is also exposed to numerous modifications.⁴ Usually, starch is modified by chemical and physical procedures or their combinations. However, generally, chemically modified starch is used in the industry.⁵

Not only macroscopic properties but also the chemical structure of the starch have been affected by these modifications.⁶ Chemical modifications result in the introduction of substituents into the starch, thus altering its basic properties, e.g. thermal stability, viscosity, and solubility molecular weight.⁷

Oxidation, esterification and etherification are three key processes, used in starch modification;⁸ however, it is worthy of mention that cross-linked starch is one of the most desired products in the industry.⁹ Cross-linked starch can be prepared by two- or poly-function cross-linkers, such as phosphates,¹⁰ bi- or tricarboxylic acid,¹¹ and boric acid,¹² which results in a great increase in the molecular weight of starch. The chemical processing with these cross-linkers leads to the stabilization of starch grain structure, as a result of consolidation with intermolecular and covalent bonds. Thus, gel synthesized from starch cross-linking is more resistant to factors such as high temperature, low pH or shear forces. Properties of the cross-linked starch mostly depend on the type of feedstock, the process of crosslinking and the arrangement of reactions.

Due to the high surface area of porous polymers, their application in the fields of adsorption, separation, clean fuel storage

and catalysis have received increasing attention in recent years.¹³ Although porous polymers can be prepared by several methods,¹⁴ ‘template synthesis’ is one of the most popular routes. However, as far as we know, there is no report where a template is used for the synthesis of nanoporous starch. In this respect, this manuscript describes a simple procedure for the preparation of nanoporous starch *via* borax, as a green and inexpensive cross-linker, in the presence of cationic, anionic, or non-ionic templates.

2. Experimental

2.1. Materials

Wheat starch, borax (Na₂B₄O₇•10H₂O), cetyltrimethylammonium bromide (CTAB), sodium dodecyl sulfate (SDS), Tween 80, methylene blue and methyl orange were purchased from Merck and used without any further purification. Ciprofloxacin was purchased from Sigma Aldrich.

2.2. Characterization

Fourier-transform infrared spectroscopy (FT-IR) spectra were recorded with Thermo Nexus 670 spectrometer to demonstrate the difference between starch and cross-linked starch in the presence and absence of a template. The specific surface area and pore diameter were calculated with the multipoint Brunauer-Emmett-Teller (BET) and Barrett, Joyner, and Halenda (BJH) methods. The morphology of nano-porous starch was observed by a high-resolution scanning electron microscopy (HRSEM). Thermo-gravimetry analysis (TGA) and differential scanning calorimetry (DSC) were performed to confirm assessment of thermal stability and possible structural changes in materials.

2.3. Preparation of Borate-cross-linked Starch

5.5 % Water-based starch mixture was prepared by dispersing 2 g starch and 4 g template (CTAB, SDS or Tween 80) in 30 mL water. The obtained mixture was heated and held at 90 °C for 20 min. The heated starch mixture was cooled to 60 °C and 60 mL

* To whom correspondence should be addressed.

E-mail: APM, a.poursattar@urmia.ac.ir / AZ, a.zamani@urmia.ac.ir



of borax solution with various concentrations (0.04, 0.08 and 0.16 g mL⁻¹) was added to the mixture (Table 1). The resulting mixture was filtered, after stirring for 2 h. The mixture was dialyzed for 3 days against water (6 × 4 L) to remove the template and lyophilized to obtain borate-cross-linked nanoporous starch.

Table 1 Abbreviation of the prepared porous starch materials.

Sample	Template	Borax concentration /g mL ⁻¹	Name
1	CTAB	0.04	st-ctab-b4
2	CTAB	0.08	st-ctab-b8
3	CTAB	0.16	st-ctab-b16
4	SDS	0.04	st-sds-b4
5	SDS	0.08	st-sds-b8
6	SDS	0.16	st-sds-b16
7	Tween 80	0.04	st-t80-b4
8	Tween 80	0.08	st-t80-b8
9	Tween 80	0.16	st-t80-b16

2.4. Batch Adsorption Experiments

Batch tests were performed to understand the dye removal capacity of the porous starch materials. In summary, in a series of beakers 50 mg of porous starch (adsorbent) were mixed with 50 mL of methylene blue (MB) or methyl orange (MO) solution while stirring at 30 °C.¹⁵ At specific time intervals, solution samples were collected, centrifuged and analyzed (at 665 nm for MB and 464 nm for MO) using a Biochrom WPA 80-3003-75 Biowave II UV-Vis spectrophotometer. This was done to monitor the residual dye concentrations in the solutions. The adsorption capacity of porous starch for dye was calculated, using Equation 1:

$$q_e = (C_0 - C_e) \frac{V}{W} \quad (1)$$

where q_e is the amount of MB or MO adsorbed (mg g⁻¹) at time of equilibrium, C_0 and C_e are the initial and final MB or MO concentrations (mg L⁻¹), V is the volume (L) of dye solution and W is the mass (mg) of the adsorbent.

Finally, the percentage of dye removal was calculated using Equation 2:

$$\% \text{ Removal} = \frac{(C_0 - C_e)}{C_0} \times 100 \quad (2)$$

2.4.1. Effect of Amount of Adsorbent

Different amounts of pure starch (st), non-templated cross-link starch (st-b8) and templated cross-linked starch were mixed with both dyes (with fixed concentration of 5 mg L⁻¹) in separate beakers. The mixture was stirred for 1 h and the product was filtered. The absorbance was measured.

2.4.2. Effect of Initial Dye Concentration

An exact amount of st-ctab-b8 (50 mg) was mixed with different concentrations (5, 10 and 25 mg L⁻¹) of 50 mL solutions of the two dyes, respectively. The mixture was stirred for 1 h and the product was filtered. The absorbance was measured.

2.4.3. Effect of Time

The effect of time on the adsorption of dye was investigated by comparing an adsorbent-adsorbate solution with a fixed dye concentration (5 mg L⁻¹) and adsorbent dosage (50 mg) at different times.

2.5. Drug Loading Experiment

Starch is a cheap polymer material with properties such as non-toxicity, biodegradability, etc., which makes it a suitable compound for pharmaceutical research.¹⁶ Nowadays, there is a lot of interest in drug delivery.¹⁷ The delivery of ciprofloxacin, as an anti-bacterial infection drug, by synthesized cross-linked starch was investigated in this study.

Solutions with concentrations 100, 200, 300, 400 and 500 mg L⁻¹ of the drug were prepared to study the drug delivery properties of synthesized porous starch. Absorbance studies were carried out using UV spectrophotometry at 271 nm (Table 5).

200 mL of 2.1×10^{-3} M drug solution was added to the beakers containing 200 mg of pure starch, synthesized cross-link starch or synthesized template cross-linked starch at room temperature. The mixture was stirred for 1.5 h, until drug loading completion. The hydrogels that formed, were filtered, rinsed with distilled water and dried overnight in an oven at 50 °C. To ensure that the hydrogels were completely dried, it was kept at room temperature.

2.6. Drug Release from Porous Starch

To simulate the human body, a pH = 7.4 phosphate buffer was prepared and used in the drug delivery studies. In this respect, 5.79 g of Na₂HPO₄ and 3.6 g of KH₂PO₄ were dissolved in 1 L deionized water. For the drug release, the dried hydrogels were added to 200 mL of phosphate buffer. After stirring at 37 °C, samples were removed and filtered, with a 0.45 µm syringe filter, at 30 min intervals. Ultraviolet absorption of these solutions was recorded in 271 nm.

3. Results and Discussion

The proposed mechanism of the porous starch formation is described in Fig. 1. Based on the soft-templating approach, co-assembly of surfactant molecules (such as CTAB) and guest species (starch) resulted in porous starch, which is obtained after the removal of the template.

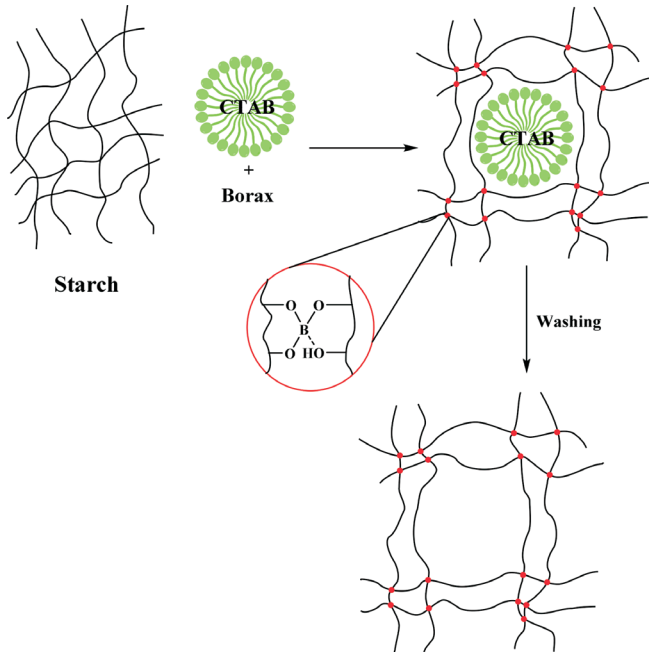


Figure 1 Schematic representation for the preparation of porous starch using CTAB as a soft template.

3.1. Synthesis and Characterization of Porous Starch

In the pure starch spectrum (Fig. 2a), the strong broad flexible vibration peak at 3411 cm⁻¹ corresponds to the bonds of the O-H

group present in the starch structure. This peak weakened in other spectrum, indicating the presence of O-B bond in response to crosslinking. Peaks of C-H stretching vibrations (about 2930 cm^{-1}) are present in all compounds (Fig. 2), indicating that the templates do not remain in the compounds. These peaks are sharp in as-synthesized templated borate-cross-linked starch (st-b8, Fig. 2c). The vibrational peak of C-O, in relation to hydroxyl groups, appeared around 1640 cm^{-1} and the asymmetric flexible vibration peaks of C-O-C appearing from 1010 to 1040 cm^{-1} in all compounds. The peaks in the 1460 cm^{-1} range correspond to C-C stretching vibrations. Due to crosslinking the peak at 1370 cm^{-1} in the starch, which is related to C-H vibrations, changed. The absorbance band at about 680 cm^{-1} is related to the O-B-O bending vibrations, which indicates the crosslinking reaction has occurred (Figs. 2d, 2e and 2f). The peaks at about 1030 – 1050 cm^{-1} in Fig. 2d, and Fig. 2e is related to the stretching of the B-O-C bonds. Therefore, the results showed that the crosslinking reaction was successful between borax and starch.

The adsorption-desorption isotherms, obtained with the BJH method, provide a suitable visual demonstration of the porous structure of the starch materials. The isotherms showed a hysteresis loop at high pressure, demonstrating the macro or nonporous system of starch materials (Fig. 3). As seen in Fig. 3, the materials exhibited type II isotherm and, H3 and H4-shaped hysteresis loop.¹⁸ All the st-t80 materials are macroporous (Fig. 3c). The hysteresis loop of st-sds-b8 isotherm showed the mesoporosity of this material (Fig. 3b) and the linear isotherm of st-ctab-b16 could be related to the presence of a broad range of meso- and macropores (Fig. 3a).

The textural properties of materials are summarized in Table 2. Material st-ctab-b8 has a BET surface area of up to $65\text{ m}^2\text{ g}^{-1}$ (Table 2, entry 2). Starch and cross-linked starch prepared in the absence of a template had the lowest surface area (8 and $10\text{ m}^2\text{ g}^{-1}$, Table 2, entries 10 and 11), which indicated that the presence of a template is critical for the synthesis of porous cross-linked starch. Also, Table 2 data (entries 2, 6 and 8) indicate that compared to Tween 80 and SDS, CTAB templated material has the highest surface area.

The HRSEM images of different starch samples at nanoscale magnification are illustrated in Fig. 4. The decrease in porosity and roughness of starch by crosslinking, is exemplified by the

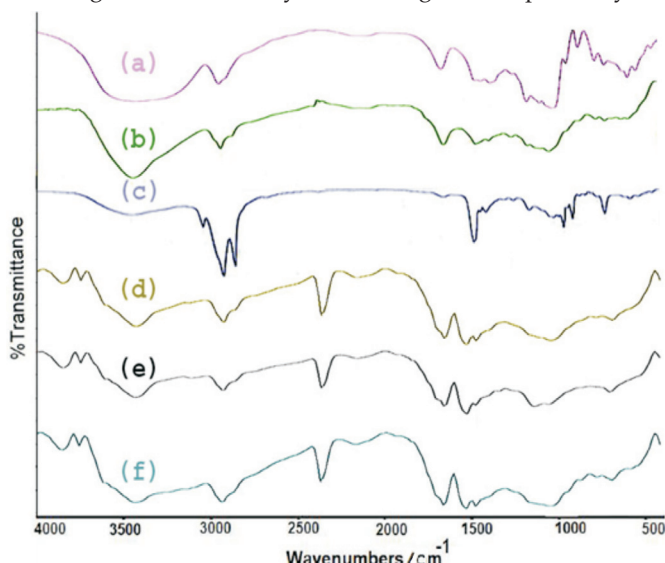


Figure 2 The near FT-IR spectra of starch (st) (a), non-templated borate-cross-linked starch (st-b8) (b), as-synthesized st-ctab-b8 (before washing) (c), st-ctab-b8 (d), st-sds-b8 (e) and st-t80-b8 (f).

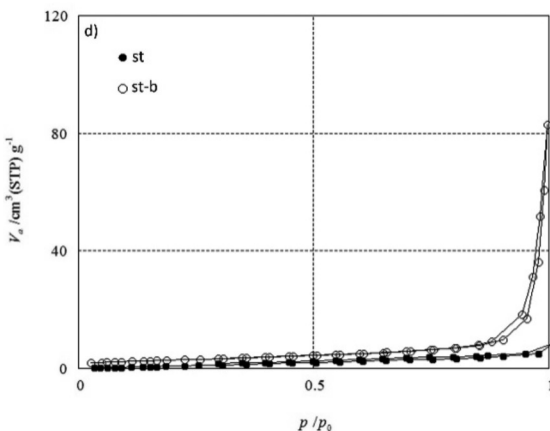
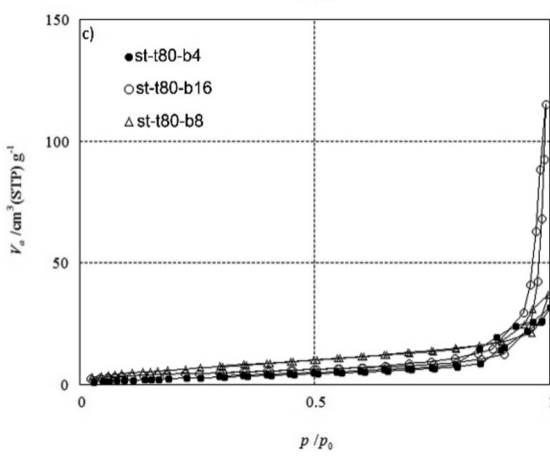
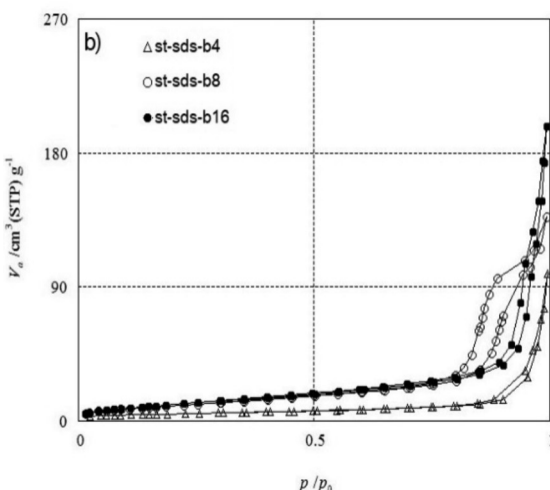
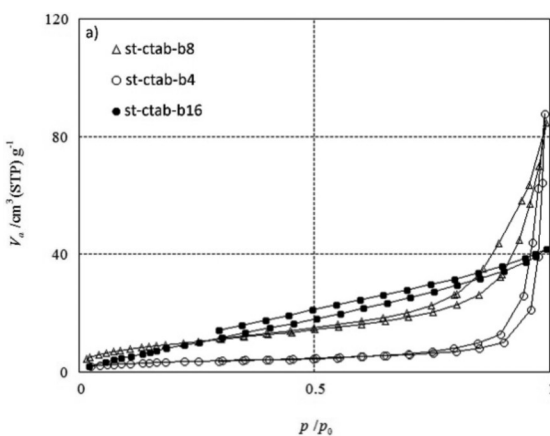


Figure 3 N_2 adsorption/desorption isotherms of st-ctab-b (a), st-sds-b (b), st-t80-b (c) and st and st-b (d).

Table 2 Textural properties of porous starch samples.

Entry	Material	BET surface area /m ² g ⁻¹	BJH pore diameter /nm
1	st-ctab-b4	13	3.6
2	st-ctab-b8	65	2.4
3	st-ctab-b16	25	2.4
4	st-sds-b4	15	4.5
5	st-sds-b8	35	2.4
6	st-sds-b16	40	2.4
7	st-t80-b4	9	2.4
8	st-t80-b8	25	2.4
9	st-t80-b16	15	2.4
10	st-b	10	2.4
11	st	8	3.2

SEM micrographs in Fig. 4a and Fig. 4b. However, the increase in porosity of materials *via* crosslinking in the presence of a template was observed in Figs. 4c–e, which agrees with data in Table 2.

The TGA graph of starch (st) (Fig. 5) shows that the degradation started at 200 °C, whereas the cross-linked starch degradation (st-b8) started at 300 °C and occurred in two stages. As a result, borax as a crosslinking agent has been able to degrade and improve the weight fraction to 100 °C and lowered the ash content in comparison with starch at the bottom. The cross-linked starch (st-ctab-b8) diagram shows that in the presence of a template the degradation occurred at approximately the same temperature of 300 °C as st-b8 over two phases and at the end some ash content remained. The degradation seen at about 200 °C is attributable to the small amount of CTAB remaining in the sample.

In starch, about 60 % of weight loss occurred at temperatures of about 200 °C and about 20 % of material remained at temperatures of about 400 °C. In st-b8 only 40 % weight loss occurred up to 300 °C and most of the weight loss occurred above 400 °C. Most of the weight loss in st-ctab-b8 occurred at 300 °C and only 20 % of the weight loss occurred at temperatures above 400 °C.

DSC analyses (Supplementary Information) is in full agreement with the TGA data. Two endothermic peaks at 100 and 230 °C in starch were related to water evaporation and melting temperature of the polymer, respectively. The exothermic peaks at 250 and 400 °C are associated with degradation temperatures. The most significant difference between the starch curve and cross-linked sample is the disappearance of the starch melting peak, which indicates that the crosslinking of starch was carried out successfully.

3.2. Nanoporous Starch Assisted Dye Removal

Recently, the use of novel methods for decolorization in many industries and water treatment has been considered.¹⁹ Methylene blue and methyl orange are the most general water-soluble pigments. So, increased concern has been concentrated on removing such pigments from wastewater. Adsorption is comparatively preferable among dye removal methods. The applicability of various adsorption kinetic models and isotherm models for dye removal by wide range of adsorbents has been reported.²⁰ This study revealed that the adsorption depends on initial dye concentration, contact time and adsorbent dosage. In this study, templated borate-cross-linked nanoporous starch was applied as an adsorbent for dyes.

Adsorbent dosage is the main process parameter, because this defines the capacity of an adsorbent for a certain amount of the adsorbate in any operating situation. Usually, the percentage of

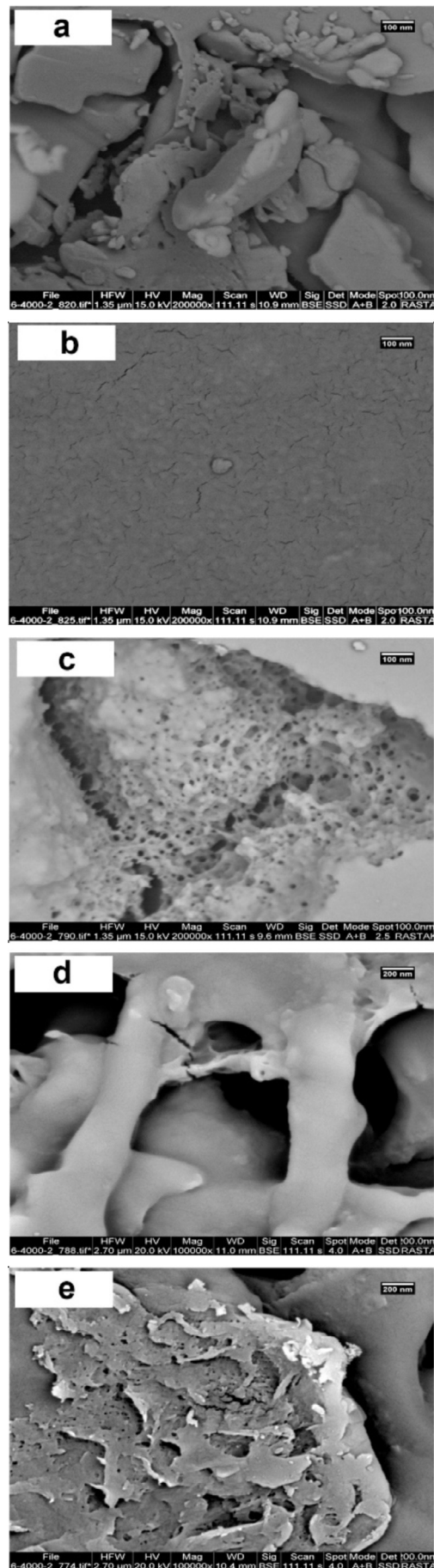


Figure 4 High resolution scanning electron microscope (HRSEM) images of st (a), st-b (b), st-ctab-b8 (c), st-sds-b8 (d) and st-t80-b8 (e).

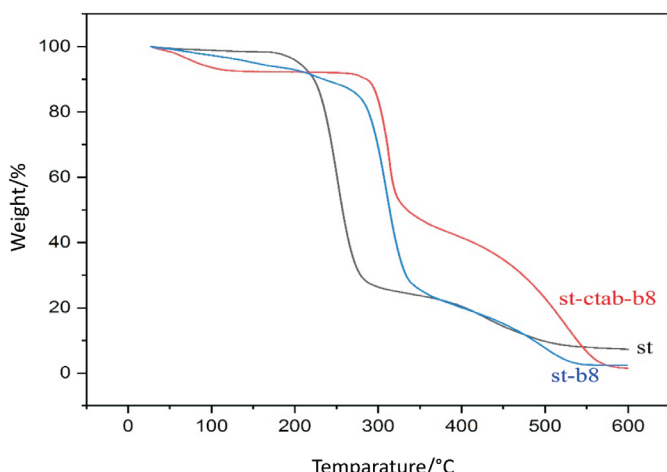


Figure 5 TGA graph of starch (st), st-b8 and st-ctab-b8.

dye elimination increases with increasing adsorbent dosage, because the number of absorption sites at the surface of adsorbent will increase with increased quantity of the adsorbent (Table 3).

The quantity of adsorption for dye elimination is directly related to the primary dye concentration. The efficacy of primary dye concentration depends on the instant connection between the dye and the vacant active sites on the adsorbent surface. Predominantly, as the primary concentration of the dye increases, the percentage of dye removal decreases, this is due to the saturation of sorption sites on the adsorbent surface. As can be seen from the results in Table 3, with increasing the amount of adsorbent at a constant concentration of dye, the percentage of adsorption increased. This increase is more evident for the CTAB template.

The effect of adsorption for different concentrations of dye was investigated. The results of the adsorption exhibited that by increasing the dye concentration the percentage of adsorption decreases (Table 4).

The effect of time is another significant parameter in dye removal. In general, the percentage of dye removal increases slightly with increasing time; however, this increase is such that most of the absorption took place in the first hour. In the second and third hour there was no noticeable absorption (Table 5).

3.3. Nanoporous Starch Assisted Control of Drug Delivery of Ciprofloxacin

The ideal drug delivery system should be comfortable, effective, biocompatible for the patient and capable of high drug loading. Porous starch meets all these conditions. An important advantage of starch polymer chains is that they are hydrolyzed to biologically acceptable compounds, so there is no need to remove the drug delivery system from the body after the active substance was released.

In this study, starch, synthesized cross-link starch and synthesized template cross-linked starch, were used to transport and release ciprofloxacin. As shown in Table 6, the template cross-linked starch illustrated a high percentage of drug release. Therefore, by measuring the percentage of drug release from the amount of adsorption at different times, it was found that the porous starch synthesized in this project was effective for the release of ciprofloxacin. Accordingly, the drug releases from hydrogels, and its concentration increases in the buffer drastically over time.

Table 3 Effect of quantity of adsorbent on dye removal.

Entry	Absorbent /mg	% Removal (MO)	q_e (MO) /mg g ⁻¹	% Removal (MB)	q_e (MB) /mg g ⁻¹
1	st (50)	42.8	2.14	56.6	2.83
2	st-b8 (50)	52	2.62	69.8	3.49
3	st-ctab-b8 (50)	82	4.14	85	4.25
4	st-sds-b8 (50)	73	3.7	77	3.85
5	st-t80-b8 (50)	72	3.6	75.4	3.77
6	st (100)	50.6	1.26	59	1.48
7	st-b8 (100)	77	1.92	78.6	1.97
8	st-ctab-b8 (100)	89.6	2.23	91.4	2.28
9	st-sds-b8 (100)	85.6	2.14	87.4	2.18
10	st-t80-b8 (100)	82	2.04	86	2.15

Table 4 Effect of dye concentration on dye removal.

Absorbent /50 mg	Dye concentration /mg L ⁻¹	% Removal (MO)	q_e (MO) /mg g ⁻¹	% Removal (MB)	q_e (MB) /mg g ⁻¹
st-ctab-b8	5	82	4.14	85	4.25
st-ctab-b8	10	62	8.81	67	8.35
st-ctab-b8	25	10	20.5	15	20.75

Table 5 Effect of time on dye removal.

Contact time (h)	% Removal (MO)	q_e (MO) /mg g ⁻¹	% Removal (MB)	q_e (MB) /mg g ⁻¹
st-ctab-b8 (1)	82	4.14	85	4.25
st-ctab-b8 (2)	83.6	4.18	86	4.3
st-ctab-b8 (3)	83.6	4.18	86.6	4.33

Table 6 Drug delivery of ciprofloxacin by st-ctab-b8.

Entry	Samples	Time intervals /min	Drug release /%
1	st	30	37
2	st	60	45
3	st	90	60
4	st-b8	30	69.8
5	st-b8	60	78
6	st-b8	90	78
7	st-ctab-b8	30	86.6
8	st-ctab-b8	60	90.3
9	st-ctab-b8	90	97.3

4. Conclusions

In summary, a green, simple and useful synthetic protocol to produce porous starch materials, using templates such as CTAB, SDS, Tween 80 and borax as cross-linkers in the aqueous phase, was presented. Most importantly, the morphological properties of the materials were characterized using N₂ adsorption/desorption porosimetry. SEM analysis confirmed the porous nature of the materials. On the other hand, the performance of porous starch materials for the removal of dyes from aqueous solution was investigated. The results show that the synthesized adsorbent would be an effective adsorbent for treating wastewater containing MO and MB. Additionally, the porous cross-linked starch was studied for its ability for the absorption and delivery of ciprofloxacin. Finally, it can be concluded that template cross-linked starch could play an important role in

removal of dye contamination from wastewater as well as a drug delivery system.

Acknowledgement

The authors are appreciatively thankful for the support provided by Urmia University.

Supplementary Material

Supplementary information is provided in the online supplement.

ORCID iDs

A. Poursattar Marjani:  orcid.org/0000-0002-5899-4285
J. Khalafy:  orcid.org/0000-0003-1202-2664

References

- 1 A. Kunkel, J. Becker, L. Börger, J. Hamprecht, S. Koltzenburg, R. Loos, M.B. Schick, K. Schlegel, C. Sinkel, G. Skupin and M. Yamamoto, Polymers, biodegradable, in *Ullmann's Encyclopedia of Industrial Chemistry*, Wiley-VCH Verlag GmbH & Co. KGaA, 2016.
- 2 a) Maulida, M. Siagian and P. Tarigan, Production of starch based bioplastic from cassava peel reinforced with microcrystalline cellulose avicel PH101 using sorbitol as plasticizer, *J. Phys.: Conf. Ser.*, 2016, **710**, 012012. b) M.K. Marichelvam, M. Jawaid and M. Asim, Corn and rice starch-based bio-plastics as alternative packaging materials, *Fibers*, 2019, **7**, 32.
- 3 Y. Nakamura, *Starch Metabolism and Structure*, Springer, Tokyo, Japan, 2015.
- 4 Q. Chen, H. Yu, L. Wang, Z. ul Abdin, Y. Chen, J. Wang, W. Zhou, X. Yang , R. Khan, H. Zhang and X. Chen, Recent progress in chemical modification of starch and its applications, *RSC Adv.*, 2015, **5**, 67459–67474.
- 5 A.V. Singh, L.K. Nath and A. Singh, Pharmaceutical, food and non-food applications of modified starches: a critical review, *EJEAFChe*, 2010, **9**, 1214–1221.
- 6 Z. Din, H. Xiong and P. Fei, Physical and chemical modification of starches – A review, *Crit. Rev. Food Sci. Nutr.*, 2017, **57**, 2691–2705.
- 7 K. Lewicka, P. Siemion and P. Kurcok, Chemical modifications of starch: microwave effect, *Int. J. Polym. Sci.*, 2015, **2015**, 867697.
- 8 a) P. Dournel, Process for the manufacture of oxidized starch, oxidized starch and its use. *US patent*, 2015, 8936820. b) S. Tian, Y. Chen, Z. Chen, Y. Yang and Y. Wang, Preparation and characteristics of starch esters and its effects on dough physicochemical properties, *J. Food Qual.*, 2018, 1395978. c) A. Gilet, C. Quettier, V. Wiatz, H. Bricout, M. Ferreira, C. Rousseau, E. Monflier and S. Tilloy, Unconventional media and technologies for starch etherification and esterification, *Green Chem.*, 2018, **20**, 1152–1168.
- 9 N. Shah, R.K. Mewada and T. Mehta, Crosslinking of starch and its effect on viscosity behavior, *Rev. Chem. Eng.*, 2016, **32**, 265–270.
- 10 H. Dong and T. Vasanthan, Amylase resistance of corn, faba bean, and field pea starches as influenced by three different phosphorylation (cross-linking) techniques, *Food Hydrocoll.*, 2020, **101**, 105506.
- 11 M.M. Hassan, N. Tucker and M.J. Le Guen, Thermal, mechanical and viscoelastic properties of citric acid-crosslinked starch/cellulose composite foams, *Carbohydr. Polym.*, 2020, **230**, 115675.
- 12 B. Khan, M.B.K. Niazi, Z. Jahan, W. Farooq, S.R. Naqvi, M. Ali, I. Ahmed and A. Hussain, Effect of ultra-violet cross-linking on the properties of boric acid and glycerol co-plasticized thermoplastic starch films, *Food Packag. Shelf Life*, 2019, **19**, 184–192.
- 13 J. Wu, F. Xu, S. Li, P. Ma, X. Zhang, Q. Liu, R. Fu, and D. Wu, Porous polymers as multifunctional material platforms toward task-specific applications, *Adv. Mater.*, 2018, **31**, 1802922.
- 14 L. Tan and B. Tan, Hypercrosslinked porous polymer materials: design, synthesis, and applications, *Chem. Soc. Rev.*, 2017, **46**, 3322–3356.
- 15 G. Uyar, H. Kaygusuz, and F.B. Erim, Methylene blue removal by alginate-clay quasi-cryogel beads, *React. Funct. Polym.*, 2016, **106**, 1–7.
- 16 B. Hartesi, Sriwidodo, M. Abdassah and A.Y. Chaerunisaa, Starch as pharmaceutical excipient, *Int. J. Pharm., Sci. Rev. Res.*, 2016, **41**, 59–64.
- 17 P.F. Builders and M.I. Arhewoh, Pharmaceutical applications of native starch in conventional drug delivery, *Starch*, 2016, **68**, 864–873.
- 18 F. Rouquerol, J. Rouquerol and K. Sing, *Adsorption by Powders and Porous Solids*, Academic Press, San Diego, 1999, pp. 18–20.
- 19 V. Katheresan, J. Kansedo and J.L.S. Yon, Efficiency of various recent wastewater dye removal methods: a review, *J. Environ. Chem. Eng.*, 2018, **6**, 4676–4697.
- 20 M.T. Yagub, T.K. Sen, S. Afroze and H.M. Ang, Dye and its removal from aqueous solution by adsorption: a review, *Adv. Colloid Interface Sci.*, 2014, **209**, 172–184.

Supplementary material to:

S. Oftadehgan, A. Poursattar Marjani, J. Khalafy and A. Zamani,

Templated Cross-linked Nanoporous Starch,

S. Afr. J. Chem., 2020, **73**, 131–136.

Templated Cross-linked Nanoporous Starch

Somayeh Oftadehgan,^a Ahmad Poursattar Marjani,^{a,*} Jabbar Khalafy^a and Asghar Zamani^{b,*}

^aDepartment of Organic Chemistry, Faculty of Chemistry, Urmia University, Urmia, Iran

^bDepartment of Nanotechnology, Faculty of Science, Urmia University, Urmia, Iran

*E-mail: a.poursattar@urmia.ac.ir / a.zamani@urmia.ac.ir

Contents:

Figure S1. DSC diagram of st

Figure S2. DSC diagram of st-b8

Figure S3. DSC diagram of st-ctab-b8

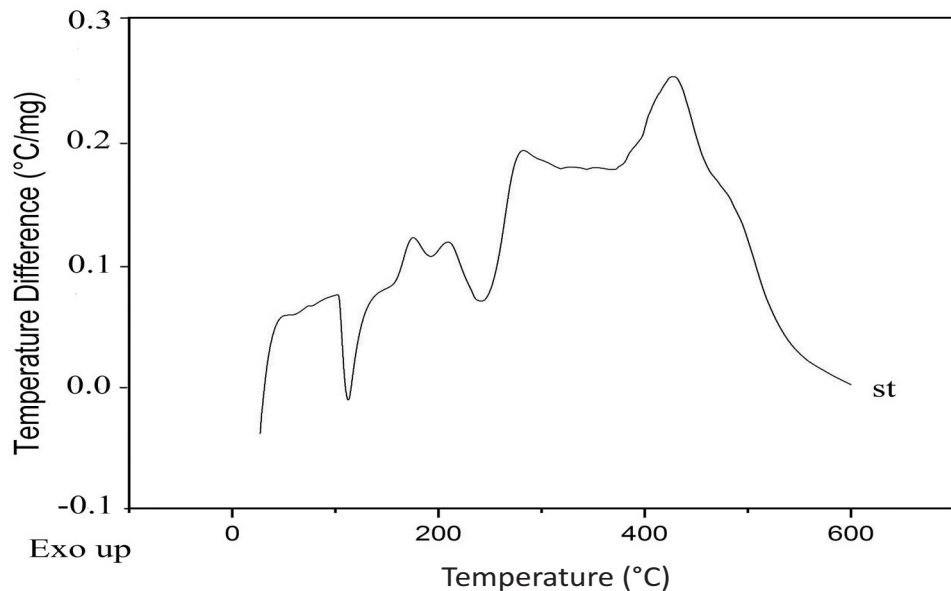


Figure S1. DSC diagram of st.

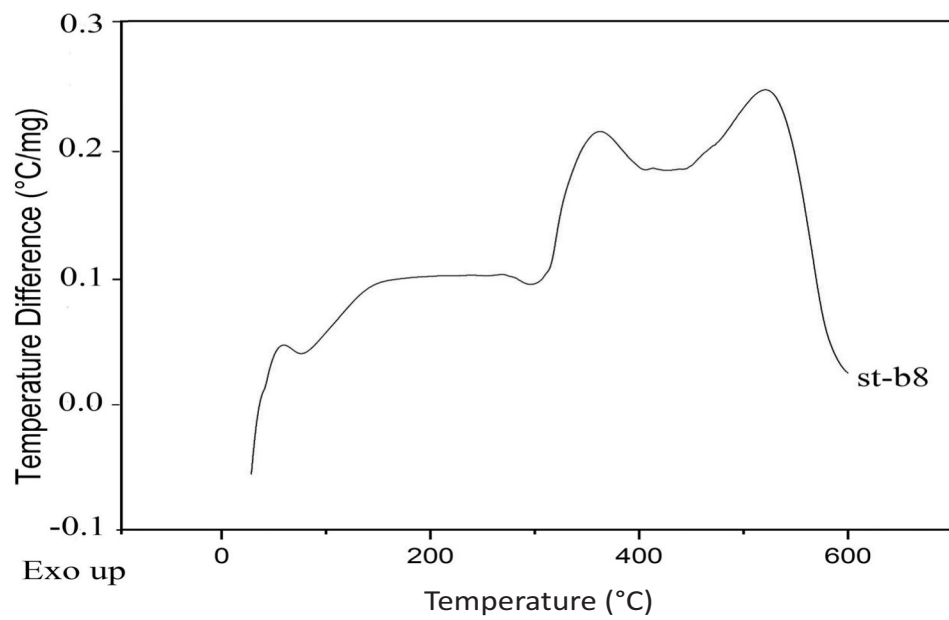


Figure S2. DSC diagram of st-b8.

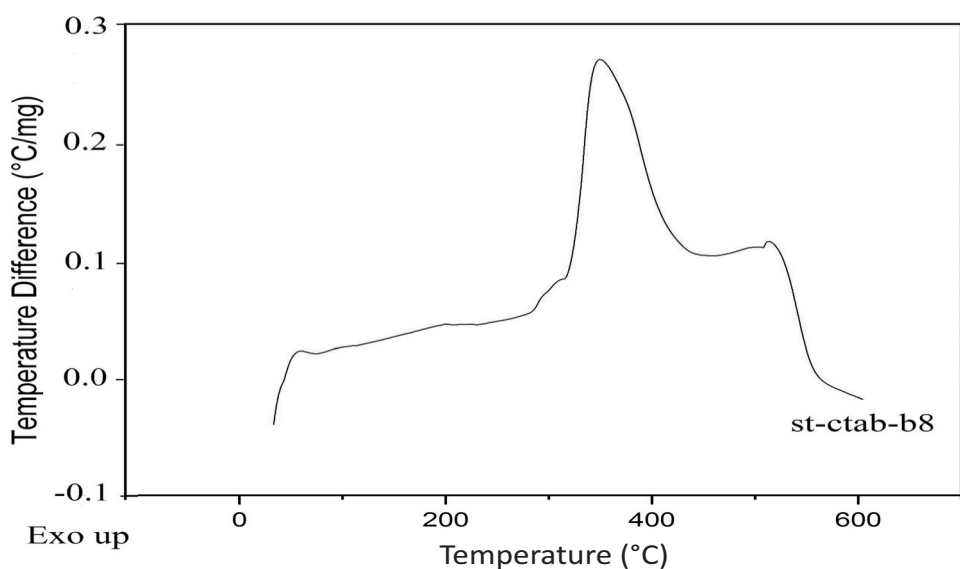


Figure S3. DSC diagram of st-ctab-b8.